J. Fluid Mech. (1968), *vol.* 34, *part* 3, *pp.* 481–495
Printed in Great Britain

Static menisci in a vertical right circular cylinder

By PAUL CONCUS

Lawrence Radiation Laboratory, University of California,
Berkeley, California 94720

(Received 20 May 1968)

The solution of the differential equation describing the equilibrium meniscus in a vertical right circular cylinder is obtained over the entire range of contact angles and Bond numbers (dimensionless ratios of gravitational to capillary forces) for which a stable meniscus exists. The first few terms of the asymptotic series valid for Bond numbers of small and large magnitude are given, and the numerical solution for intermediate values is computed. The behaviour of the solution as a function of contact angle and Bond number is depicted graphically.

1. Introduction

A few years ago White & Tallmadge (1965) calculated the shape of static menisci on the outside of a vertical right circular cylinder for a perfectly wetting fluid (zero-degree contact angle). The corresponding problem for static menisci inside a cylinder for both zero and more general contact angles has stimulated interest for many years—early references date back as far as Laplace (1805). Rayleigh (1916) gave expressions for the asymptotic solutions for very small and very large cylinders, primarily for zero-degree contact angle; and Bashford & Adams (1883) and Runge (1895) performed some of their early work in the numerical solution of differential equations by calculating meniscus shapes. In recent years the advent of space exploration and the accompanying interest in low-gravity environments have revived the study of these shapes. Reynolds & Satterlee (1966) give additional information on the solution of the interior meniscus problem which includes graphs depicting stability and some of the geometric properties of the interfaces over a large range of parameters. A number of other authors have also studied aspects of this problem recently, and most of their work can be found listed in the bibliographies of Habip (1965), Lockheed Missiles and Space Co. (1967), and Reynolds & Satterlee (1966).

The purpose of this paper is to complete the description of the equilibrium meniscus in a vertical right circular cylinder for all values of the two basic parameters, the contact angle between the meniscus and the cylinder wall and the Bond number (a dimensionless parameter that is the ratio of gravitational to capillary forces). Asymptotic solutions along with their range of validity are derived for small and large magnitudes of the Bond number and the numerical solution is obtained for intermediate values. The range of validity of the asymptotic solutions is found by comparison with the numerical solution, and the

dependence of the solution on contact angle and Bond number is depicted graphically. Conditions for meniscus stability are also discussed. The attempt to make the results presented here complete will necessitate presentation of some results that overlap those presented by others elsewhere. The reader is referred to Reynolds & Satterlee for a discussion of the relevant background material.

2. Mathematical description

The equilibrium free surface of a liquid inside a vertical cylinder of circular cross-section (figure 1) satisfies the differential equation

$$\frac{1}{r}\frac{d}{dr}\left[\frac{rdf(r)/dr}{[1+(df(r)/dr)^2]^{\frac{1}{2}}}\right]-Bf(r)-\lambda=0 \quad (0<r<1), \tag{1}$$

with the boundary conditions

$$df(r)/dr = 0 \quad \text{at} \quad r = 0 \tag{2a}$$

and

$$df(r)/dr = \cot\theta \quad \text{at} \quad r = 1. \tag{2b}$$

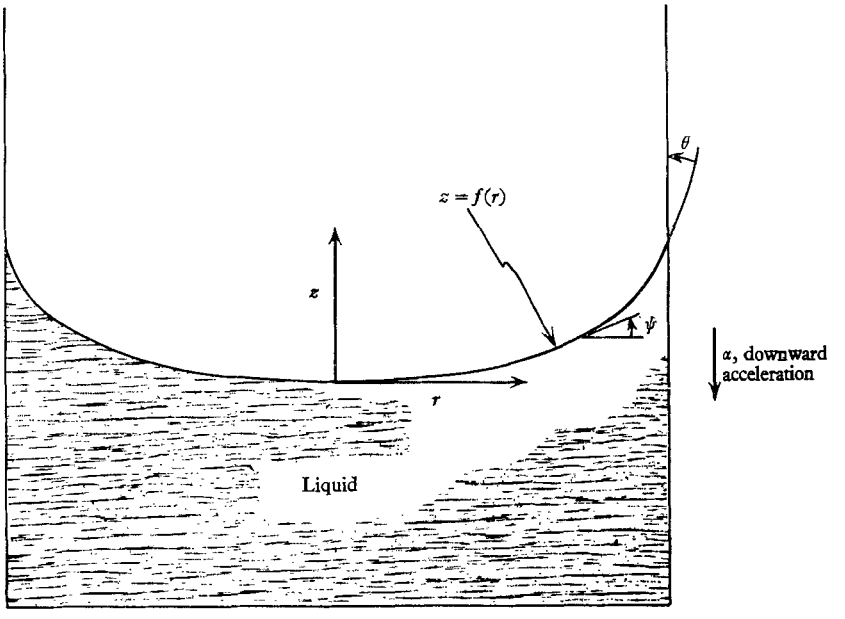

FIGURE 1. Physical configuration.

The quantities f, r, B and λ are dimensionless, where $B = \rho\alpha a^2/\sigma$ is the Bond number with ρ the liquid density, α the vertical acceleration field (positive downward), a the radius of the cylinder, and σ the surface tension; ar is the radial distance from the axis; $af(r)$ is the height of the surface at a point r; and θ is the given contact angle between the surface and the cylinder wall. Let the origin of the co-ordinate system be at the centre of the free surface, that is, apply the

additional boundary condition

$$f(0) = 0; \tag{3}$$

then the unknown parameter λ is twice the mean curvature of the surface at $r = 0$, or, what is the same thing, twice the curvature of $f(r)$ at $r = 0$. The parameter λ is related to the pressure difference across the surface by $\lambda = a(p_O - p_L)/\sigma$, where p_O is the pressure outside the liquid and p_L is the pressure in the liquid at $r = 0$ just below the interface. Since (1) and (2) are invariant with respect to the transformation

$$\bar{f} = f + h, \quad \bar{\lambda} = \lambda - Bh,$$

the height of the meniscus centre in a capillary tube above the free plane level of a reservoir in which the tube is immersed for $B > 0$ is $h = a\lambda/B$.

Observe that the solution to (1), (2) and (3) for a non-wetting fluid ($\frac{1}{2}\pi < \theta \leqslant \pi$) can be obtained directly from that for a wetting fluid ($0 \leqslant \theta < \frac{1}{2}\pi$) by replacing f by $-f$, λ by $-\lambda$, and θ by $(\pi - \theta)$. Thus it is necessary to obtain the solution only for a wetting fluid, which is the case considered in the remainder of the paper. For the case in which $\theta = \frac{1}{2}\pi$, the solution is, of course, the trivial one of the flat interface $f(r) \equiv 0$, for which $\lambda = 0$.

It is convenient to have (1), (2) and (3) also expressed in parametric form in terms of the parameter $\psi = \tan^{-1}(df/dr)$, the angle between the surface and the horizontal. The equations are

$$\frac{df(\psi)}{d\psi} = \frac{\sin\psi}{D}, \quad \frac{dr(\psi)}{d\psi} = \frac{\cos\psi}{D}, \quad (0 < \psi < \tfrac{1}{2}\pi - \theta), \tag{4}$$

where $D = Bf - (\sin\psi)/r + \lambda$, with the boundary conditions

$$f(\psi) = r(\psi) = 0 \quad \text{at} \quad \psi = 0 \tag{5}$$

and

$$r(\psi) = 1 \quad \text{at} \quad \psi = \tfrac{1}{2}\pi - \theta. \tag{6}$$

Equation (1) can also be written in terms of the parameter ψ as

$$\frac{1}{r}\frac{d}{dr}(r\sin\psi) - Bf - \lambda = \cos\psi\frac{d\psi}{dr} + \frac{\sin\psi}{r} - Bf - \lambda = 0. \tag{7}$$

The quantity $\cos\psi\, d\psi/dr$ is the curvature of $f(r)$, and $(\sin\psi)/r$ is the other principal curvature of the free surface. Notice that the denominator D in (4) is just the curvature of $f(r)$.

The only solutions to the above equations that are considered here are those that are stable and physically realizable. It can be shown that these solutions are characterized as follows for $0 < \theta < \frac{1}{2}\pi$. First, λ is positive. Secondly, (*a*) for $B > 0$, the curvature of $f(r)$ increases monotonically from its value of $\frac{1}{2}\lambda$ at $r = 0$ to its maximal value at the wall, and hence f, r and ψ also increase monotonically from the centre to the wall. There are other solutions which loop back on themselves one or more times between $r = 0$ and the wall and satisfy the boundary conditions (to within multiples of 2π), but these are, in general, unstable and not physically realizable; (*b*) for $B < 0$, the curvature of $f(r)$ decreases monotonically from its value of $\frac{1}{2}\lambda$ at $r = 0$ to its minimal non-negative value at

the wall, and hence f, r and ψ increase monotonically from the centre to the wall. For each contact angle there is a critical (negative) value of B, $B_{cr}(\theta)$, which is the least value of B for which such a solution is possible. For values of B less than B_{cr} there are undulating solutions of (4) satisfying the boundary conditions, but computational results indicate that these are unstable (see §6); the solution, $f(r)$, for the critical value of B has the property that its curvature decreases to zero at the wall.

3. Asymptotic solution for small B

The asymptotic solution of (4), (5) and (6) for $|B| \ll 1$ can be obtained by a formal perturbation expansion in powers of B by letting

$$\left.\begin{aligned} f(\psi) &= f_0(\psi) + Bf_1(\psi) + O(B^2), \\ r(\psi) &= r_0(\psi) + Br_1(\psi) + O(B^2), \\ \text{and} \qquad \lambda &= \lambda_0 + B\lambda_1 + O(B^2), \end{aligned}\right\} \tag{8}$$

as B approaches zero.† Substitution into (4) yields the zero-order equations

$$\frac{df_0}{d\psi} = \frac{\sin\psi}{\lambda_0 - (\sin\psi)/r_0}, \quad \frac{dr_0}{d\psi} = \frac{\cos\psi}{\lambda_0 - (\sin\psi)/r_0}, \quad (0 < \psi < \tfrac{1}{2}\pi - \theta).$$

The solution, subject to the boundary conditions (5) and (6) with subscript zero on the variables, is the spherical segment

$$\left.\begin{aligned} f_0 &= 2(1-\cos\psi)/\lambda_0 = \sec\theta(1-\cos\psi) \\ r_0 &= 2(\sin\psi)/\lambda_0 = \sec\theta\sin\psi \\ \lambda_0 &= 2\cos\theta. \end{aligned}\right\}, \quad (0 \leqslant \psi \leqslant \tfrac{1}{2}\pi - \theta), \tag{9}$$

This is the solution for zero Bond number (zero gravity).

Using the above zero-order solution, one then obtains the equations for the first-order quantities,

$$\begin{aligned} df_1/d\psi &= -\sin\psi[r_1\csc\psi + \sec^3\theta(1-\cos\psi) + \lambda_1\sec^2\theta], \\ dr_1/d\psi &= -\cos\psi[r_1\csc\psi + \sec^3\theta(1-\cos\psi) + \lambda_1\sec^2\theta], \quad (0 < \psi < \tfrac{1}{2}\pi - \theta). \end{aligned}$$

The solution, subject to the appropriate first-order boundary conditions, (5) with subscript one, and, instead of (6),

$$r_1(\psi) = 0 \quad \text{at} \quad \psi = \tfrac{1}{2}\pi - \theta,$$

is

$$\left.\begin{aligned} f_1 &= \sec^3\theta\left[-\frac{1}{6} + \frac{\cos\psi}{2} - \frac{\cos^2\psi}{3} + \tfrac{1}{3}\log\left(\frac{1+\cos\psi}{2}\right) - \lambda_1\cos\theta\,\frac{1-\cos\psi}{2}\right], \\ r_1 &= -\sec^3\theta\left[\tfrac{1}{2}\sin\psi - \frac{1-\cos^3\psi}{3\sin\psi} + \frac{\lambda_1}{2}\cos\theta\sin\psi\right], \\ \lambda_1 &= -\sec\theta + \tfrac{2}{3}\sec^3\theta(1-\sin^3\theta). \end{aligned}\right\} \tag{10}$$

† Expanding not only f and r but also λ results in a solution that is somewhat more convenient to use than the one Rayleigh obtained by expanding only f and r.

Substitution of (9) and (10) into (8) then gives the desired asymptotic solution. The magnitude of B up to which this solution for small $|B|$ remains sufficiently accurate is discussed in §6.

Expressions for the surface area and volume valid for small $|B|$ can be obtained by using the above solutions for f and r. The surface area, S, of the equilibrium free surface is

$$S = \int_0^{\frac{1}{2}\pi-\theta} 2\pi r \frac{dr}{d\psi} \sec\psi \, d\psi,$$

which for small $|B|$ becomes

$$S = 2\pi(1-\sin\theta)\sec^3\theta\{\cos\theta - B[\lambda_1 + \sec\theta(1-\sin\theta)/2] + O(B^2)\}.$$

The volume, V, of liquid between the horizontal plane $z = 0$ and the free surface is

$$V = \int_0^{\frac{1}{2}\pi-\theta} 2\pi r f \frac{dr}{d\psi} \, d\psi,$$

which for small $|B|$ is

$$V = \pi\{-\lambda_1 + B\sec^5\theta[-(\tfrac{4}{3}+\tfrac{3}{2}\lambda_1\cos\theta)\cos^2\theta + (1-\sin\theta)/3 + (\tfrac{5}{3}+\lambda_1\cos\theta)(1-\sin^3\theta) - \tfrac{2}{3}\cos^2\theta(1+\sin^2\theta) + \tfrac{1}{3}\cos^2\theta\log((1+\sin\theta)/2)] + O(B^2)\}.$$

4. Asymptotic solution for large B

Since B_{cr}, the critical value of B less than which a stable free surface does not exist, is a negative number of only moderate magnitude for all contact angles (see Reynolds & Satterlee, figure 11.23, p. 408), it is not necessary to consider an asymptotic solution for negative values of B of large magnitude. The asymptotic solution developed here is for large positive values of B, only.

The asymptotic solution for $B \gg 1$ is found by using a boundary-layer technique. One assumes that there is a central core region covering most of the cylinder in which $df/dr = \tan\psi$ is small, and a boundary-layer region near the wall in which ψ increases rapidly to its given boundary value. Matching the core and boundary-layer solutions in the transition zone between them determines the value of the constant, λ.

In the core region ($\psi \ll 1$), the solution is most easily found from (1), which for small ψ becomes

$$\frac{1}{r_c}\frac{d}{dr_c}\left\{r_c\frac{df_c}{dr_c}[1+O(\psi^2)]\right\} - Bf_c - \lambda = 0, \tag{11}$$

where the subscript c denotes the core region. The solution, subject to ($2a$) and (3), is

$$f_c = \lambda B^{-1}[I_0(B^{\frac{1}{2}}r_c) - 1][1+O(\psi^2)], \tag{12}$$

from which the relationship between r_c and ψ is found to be

$$\psi = \lambda B^{-\frac{1}{2}} I_1(B^{\frac{1}{2}}r_c)[1+O(\psi^2)],$$

where I_0 and I_1 are modified Bessel functions of order zero and one, respectively.

The solution in the boundary-layer region is obtained by first estimating the boundary-layer thickness, which is assumed to be of the order of B^{-m}, where m is a positive exponent to be determined. That is, let x be the boundary-layer variable, where

$$x = B^m(1-r) \tag{13}$$

is of order one in the boundary layer. Then substitution into (7) yields

$$B^m \frac{d\psi}{dx}\cos\psi + \frac{\sin\psi}{1-B^{-m}x} - Bf - \lambda = 0. \tag{14}$$

In order that $\psi = \tan^{-1}(df/dr) = -B^m \tan^{-1}(df/dx)$ be of order one in the boundary layer, it is necessary that f be of order B^{-m}.† The quantity m is determined by requiring that the dominant capillary term—the first term in (14), which is the one due to the curvature of $f(r)$—and the gravitational term, the third term in (14), be of the same order. This yields the relationship

$$B^m = B^{1-m},$$

so that the proper choice for m is $m = \frac{1}{2}$.

One thus seeks a solution in the boundary-layer region of the form

$$f_b(\psi) = \epsilon F_1(\psi) + \epsilon^2 F_2(\psi) + O(\epsilon^3), \tag{15a}$$

$$r_b(\psi) = 1 - \epsilon x_1(\psi) - \epsilon^2 x_2(\psi) + O(\epsilon^3), \tag{15b}$$

where $\epsilon = B^{-\frac{1}{2}}$ is the expansion parameter and $f_b(\psi)$ and $r_b(\psi)$ are the solutions for $f(\psi)$ and $r(\psi)$, respectively, in the boundary layer. The expansion is carried out to ϵ^2 so that the terms up to order B^{-1} are included, in a sense paralleling (8), the expansion for small $|B|$, where terms up to order B are included. The appropriate boundary conditions are the ones corresponding to (6),

$$x_1(\psi) = x_2(\psi) = 0 \quad \text{at} \quad \psi = \tfrac{1}{2}\pi - \theta, \tag{16}$$

and, in addition, the ones that outside the boundary layer f_b approach zero with ψ,

$$F_1(\psi) = F_2(\psi) = 0 \quad \text{at} \quad \psi = 0. \tag{17}$$

In obtaining the solution it is assumed that λ is negligible in comparison with terms of order one, an assumption that is verified after the solution is found.

Substituting (15) into (4) yields the first-order equations (terms of order ϵ)

$$dF_1/d\psi = \sin\psi/F_1, \quad dx_1/d\psi = -\cos\psi/F_1.$$

The solution, subject to the conditions (16) and (17), is

$$\left.\begin{aligned} F_1 &= 2\sin\tfrac{1}{2}\psi, \\ x_1 &= \log[\tan\tfrac{1}{4}\psi_1/\tan\tfrac{1}{4}\psi] + 2\cos\tfrac{1}{2}\psi_1 - 2\cos\tfrac{1}{2}\psi, \end{aligned}\right\} \tag{18}$$

† It is assumed, of course, that the given contact angle θ requires that ψ be of order one at the boundary. If θ is close to $\frac{1}{2}\pi$, then a boundary-layer solution is not necessary, and the core solution may be used all the way to the wall.

where ψ_1 is the value of ψ at the wall,

$$\psi_1 = \tfrac{1}{2}\pi - \theta. \tag{19}$$

The second-order equations (terms of order ϵ^2) are

$$\frac{dF_2}{d\psi} = -\frac{\sin\psi}{F_1^2}F_2 + \frac{\sin^2\psi}{F_1^2},$$

$$\frac{dx_2}{d\psi} = \frac{\cos\psi}{F_1^2}F_2 - \frac{\sin\psi\cos\psi}{F_1^2},$$

where F_1 is given by (18). The solution, subject to conditions (16) and (17), is

$$\begin{aligned} F_2 &= \frac{2}{3}\frac{1-\cos^3\tfrac{1}{2}\psi}{\sin\tfrac{1}{2}\psi}, \\ x_2 &= -\tfrac{2}{3}\sin^2\tfrac{1}{2}\psi_1 - \tfrac{1}{6}(1+\cos\tfrac{1}{2}\psi_1)^{-1} + \tfrac{1}{2}\log\frac{\tan\tfrac{1}{4}\psi_1}{\tan\tfrac{1}{4}\psi} \\ &\quad + \tfrac{2}{3}\sin^2\tfrac{1}{2}\psi + \tfrac{1}{6}(1+\cos\tfrac{1}{2}\psi)^{-1}. \end{aligned} \tag{20}$$

Equations (18) and (20), when substituted into (15), then give the desired boundary-layer solution.

The value of λ appearing in the core solution (12) is evaluated by matching the core and boundary-layer solutions in the region of transition between the two, that is, far enough from the wall so that ψ is of order ϵ, but close enough so that $(1-r) \ll 1$. In terms of the expansion parameter ϵ the core solution (12) in the transition region is

$$f_c = \epsilon^2\lambda[I_0(r_c/\epsilon) - 1][1 + O(\epsilon^2)].$$

In this region r_c is close to one, so that the Bessel function in the above expression may be approximated by its asymptotic expansion for large argument to yield

$$f_c = \epsilon^2\lambda\frac{\exp(r_c/\epsilon)}{(2\pi r_c/\epsilon)^{\frac{1}{2}}}\left[1 + \frac{\epsilon}{8r_c} + O(\epsilon^2)\right]. \tag{21}$$

The asymptotic expression for the boundary-layer solution in the transition region is found by using the forms that (18) and (20) take for small ψ,

$$\begin{aligned} F_1 &= \psi + O(\psi^3), \\ x_1 &= -\log\tfrac{1}{4}\psi + \log\tan\tfrac{1}{4}\psi_1 + 2\cos\tfrac{1}{2}\psi_1 - 2 + O(\psi^2), \\ F_2 &= \tfrac{1}{2}\psi + O(\psi^3), \\ x_2 &= -\tfrac{1}{2}\log\tfrac{1}{4}\psi - \tfrac{2}{3}\sin^2\tfrac{1}{2}\psi_1 \\ &\quad - \tfrac{1}{6}[1+\cos\tfrac{1}{2}\psi_1]^{-1} + \tfrac{1}{2}\log\tan\tfrac{1}{4}\psi_1 + \tfrac{1}{12} + O(\psi^2). \end{aligned}$$

Substituting these equations into (15) and taking ψ to be the same order as ϵ yields

$$f_b(\psi) = \epsilon\psi + \tfrac{1}{2}\epsilon^2\psi + O(\epsilon^4) \tag{22a}$$

and

$$\begin{aligned} 1 - r_b(\psi) &= \epsilon(1+\tfrac{1}{2}\epsilon)(-\log\tfrac{1}{4}\psi + \log\tan\tfrac{1}{4}\psi_1) - 2\epsilon(1-\cos\tfrac{1}{2}\psi_1) \\ &\quad + \epsilon^2[\tfrac{1}{12} - \tfrac{2}{3}\sin^2\tfrac{1}{2}\psi_1 - \tfrac{1}{6}(1+\cos\tfrac{1}{2}\psi_1)^{-1}] + o(\epsilon^2). \end{aligned} \tag{22b}$$

Note that the remainder term in (22*b*) is evidently of the form $O(\epsilon^3 \log \psi)$, which for $\psi = O(\epsilon)$ is $o(\epsilon^2)$, but larger than $O(\epsilon^3)$. In the transition region $1 - r_b(\psi)$ is $O(\epsilon \log \epsilon)$, and the error in (15*b*) increases to $O(\epsilon^3 \log \epsilon)$ from its value of $O(\epsilon^3)$ in the boundary layer.

Exponentiation of (22*b*) yields

$$\psi = 4 \exp \{\log \tan \tfrac{1}{4}\psi_1 - (1 - r_b(\psi))/\epsilon - 2(1 - \cos \tfrac{1}{2}\psi_1) + \tfrac{1}{2}[1 - r_b(\psi)] + \epsilon[\tfrac{13}{12} - \cos \tfrac{1}{2}\psi_1 - \tfrac{2}{3} \sin^2 \tfrac{1}{2}\psi_1 - \tfrac{1}{6}(1 + \cos \tfrac{1}{2}\psi_1)^{-1}] + o(\epsilon)\}.$$

Substitution of this equation into (22*a*) and simplifying yields

$$f_b(\psi) = 4\epsilon\{1 + \tfrac{1}{2}[1 - r_b(\psi)] + \epsilon[\tfrac{19}{12} - \cos \tfrac{1}{2}\psi_1 - \tfrac{2}{3} \sin^2 \tfrac{1}{2}\psi_1 - \tfrac{1}{6}(1 + \cos \tfrac{1}{2}\psi_1)^{-1}] + o(\epsilon)\} \times \exp [-(1 - r_b(\psi))/\epsilon + \log \tan \tfrac{1}{4}\psi_1 - 2(1 - \cos \tfrac{1}{2}\psi_1)].$$

The core solution (21) may now be matched to the above boundary-layer solution by setting $r_c = r_b$ and equating f_c to f_b. The result, after the relation $[1 - r_b(\psi)] = O(\epsilon \log \epsilon)$ has been used to expand (21) as

$$f_c = (2\pi)^{-\frac{1}{2}} \lambda \epsilon^{\frac{5}{2}} \exp (r_c/\epsilon)[1 + \tfrac{1}{2}(1 - r_c) + \tfrac{1}{8}\epsilon + o(\epsilon)],$$

is the expression for λ,

$$\lambda = e^{-1/\epsilon} \epsilon^{-\frac{3}{2}} \lambda_0 (1 + \epsilon \lambda_1 + o(\epsilon)), \tag{23}$$

where $$\lambda_0 = 4(2\pi)^{\frac{1}{2}} \tan \tfrac{1}{4}\psi_1 \exp \{-2[1 - \cos \tfrac{1}{2}\psi_1]\}$$

and $$\lambda_1 = \tfrac{35}{24} - \cos \tfrac{1}{2}\psi_1 - \tfrac{2}{3} \sin^2 \tfrac{1}{2}\psi_1 - \tfrac{1}{6}[1 + \cos (\tfrac{1}{2}\psi_1)]^{-1}.$$

Examination of (23) shows it to be consistent with the assumption made previously that λ is small compared with terms of order one.

The asymptotic expressions for large B for the surface area S of the equilibrium free surface and the volume V of liquid between the horizontal plane $z = 0$ and the free surface are then found to be

$$S = \pi\{1 + 4\epsilon[1 - \cos \tfrac{1}{2}\psi_1] + O(\epsilon^2)\}$$

and

$$V = 2\pi\epsilon^2 \sin \psi_1 + O(\epsilon^3).$$

5. Numerical solution

The solutions for large B and for values of B near zero can be found by using the asymptotic expressions given in the previous sections. For intermediate values of B it is necessary to solve numerically the boundary-value problem describing the free surface. This is accomplished here by using the initial-value, or shooting, method (see Fox 1962, pp. 63–4). Equation (4) is integrated, using (5) and a guessed value of λ as initial conditions, until $\psi = \frac{1}{2}\pi - \theta$, at which point the right-hand boundary condition (6) is, in general, not satisfied. The value of λ is then adjusted, by using Newton's method, and the process repeated until (6) is satisfied to the desired accuracy. The specific equation used to correct λ is

$$\lambda_{n+1} = \lambda_n - \frac{r - 1}{\partial r/\partial \lambda}\bigg|_{\substack{\lambda = \lambda_n \\ \psi = \frac{1}{2}\pi - \theta}},$$

where λ_n denotes the nth approximation to λ; the value of $\partial r/\partial\lambda$ is obtained by simultaneously integrating the equations obtained by differentiating (4) with respect to λ,

$$\frac{\partial}{\partial\psi}\left(\frac{\partial r}{\partial\lambda}\right) = -\frac{\cos\psi}{D^2}\left(B\frac{\partial f}{\partial\lambda}+\frac{\sin\psi}{r^2}\frac{\partial r}{\partial\lambda}+1\right),$$

$$\frac{\partial}{\partial\psi}\left(\frac{\partial f}{\partial\lambda}\right) = -\frac{\sin\psi}{D^2}\left(B\frac{\partial f}{\partial\lambda}+\frac{\sin\psi}{r^2}\frac{\partial r}{\partial\lambda}+1\right),$$

along with (4), subject to the initial conditions

$$\frac{\partial r}{\partial\lambda} = \frac{\partial f}{\partial\lambda} = 0 \quad \text{at} \quad \psi = 0.$$

The numerical integration was carried out by using ZAM, a Radiation Laboratory computer library subroutine, which employs a variable-step size fourth-order Adams–Moulton method. To start the integration at $r = 0$, the presence of the terms involving $(\sin\psi)/r$ and $(\sin\psi)/r^2$ requires that an asymptotic solution be used. The asymptotic solution for small ψ for $B > 0$ is given by (12); for $B < 0$ it is

$$f = -\lambda B^{-1}\{1 - J_0[(-B)^{\frac{1}{2}}r]\}, \quad \psi = \lambda(-B)^{-\frac{1}{2}}J_1[(-B)^{\frac{1}{2}}r]. \tag{24}$$

These asymptotic solutions are used for ψ up to a value of less than 0·1 degree, at which point the numerical integration is begun.

The determination of the critical Bond number and the corresponding numerical integration for f and r require special attention, since the choice of ψ as the independent variable does not permit the integration to be carried out all the way to the wall, where the denominator D of (4) vanishes. The integration is accomplished by letting D be the independent variable, once it becomes small, and then continuing the integration of

$$\left.\begin{aligned}\frac{df}{dD} &= \frac{\sin\psi}{B\sin\psi+(\cos\psi/r)[(\sin\psi/r)-D]},\\ \text{and}\qquad \frac{dr}{dD} &= \frac{\cos\psi}{B\sin\psi+(\cos\psi/r)[(\sin\psi/r)-D]},\end{aligned}\right\} \tag{25}$$

until $D = 0$. The solution is then rescaled so that $r = 1$ at the right-hand end-point, and the shooting method correction on λ determined to make $\psi = \frac{1}{2}\pi - \theta$ when $D = 0$, rather than to make $r = 1$ when $\psi = \frac{1}{2}\pi - \theta$.

6. Results and conclusions

The solution properties are depicted in figures 2 to 5, where $f(\frac{1}{2}\pi - \theta)$, the height of the free surface at the wall, S, the area of the free surface, V, the volume of liquid between the free surface and the plane $z = 0$ and λ, twice the mean curvature of the free surface at $r = 0$, are displayed, respectively. The solid portions of the curves depict the asymptotic solutions obtained for large and

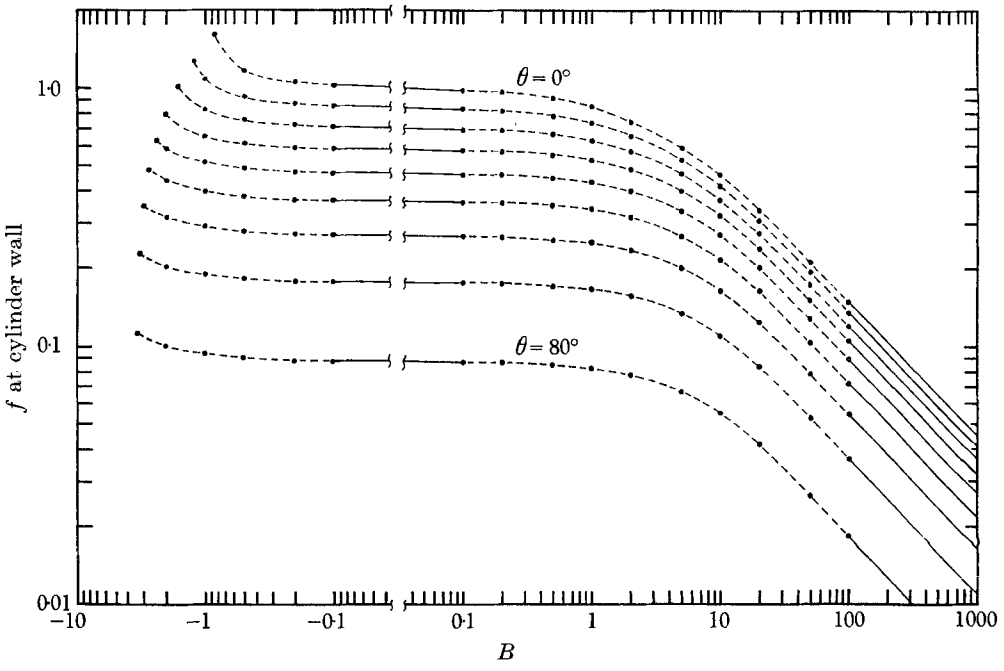

FIGURE 2. $f(\frac{1}{2}\pi - \theta)$, meniscus height at the cylinder wall, *vs.* B, Bond number. The curves in order from top to bottom are for contact angles θ = 0, 10, 20, 30, 40, 50, 60, 70 and 80 degrees.

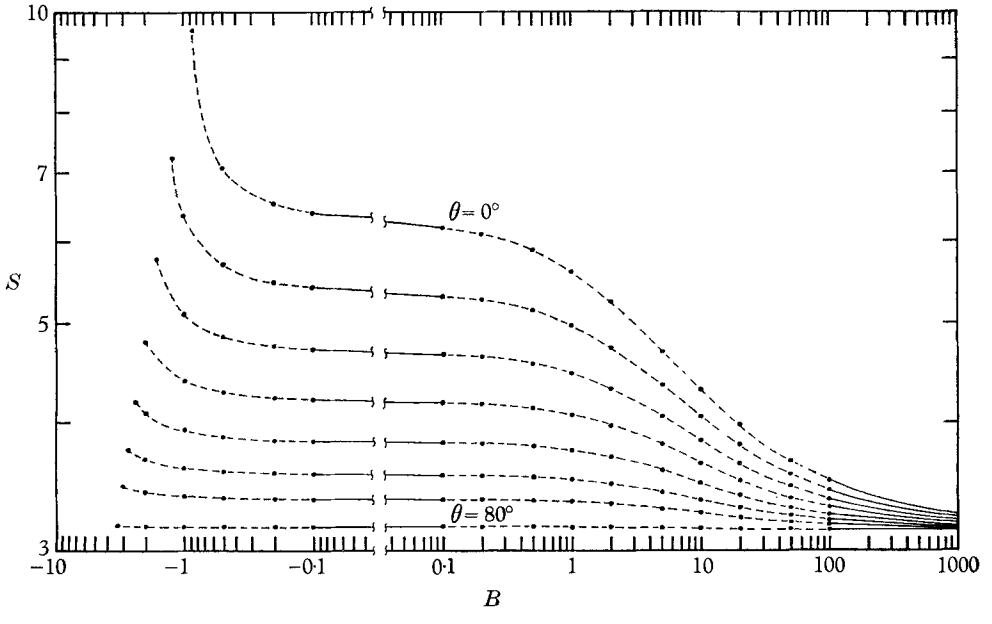

FIGURE 3. S, meniscus area, *vs.* B, Bond number. The curves in order from top to bottom are for contact angles θ = 0, 10, 20, 30, 40, 50, 60 and 80 degrees.

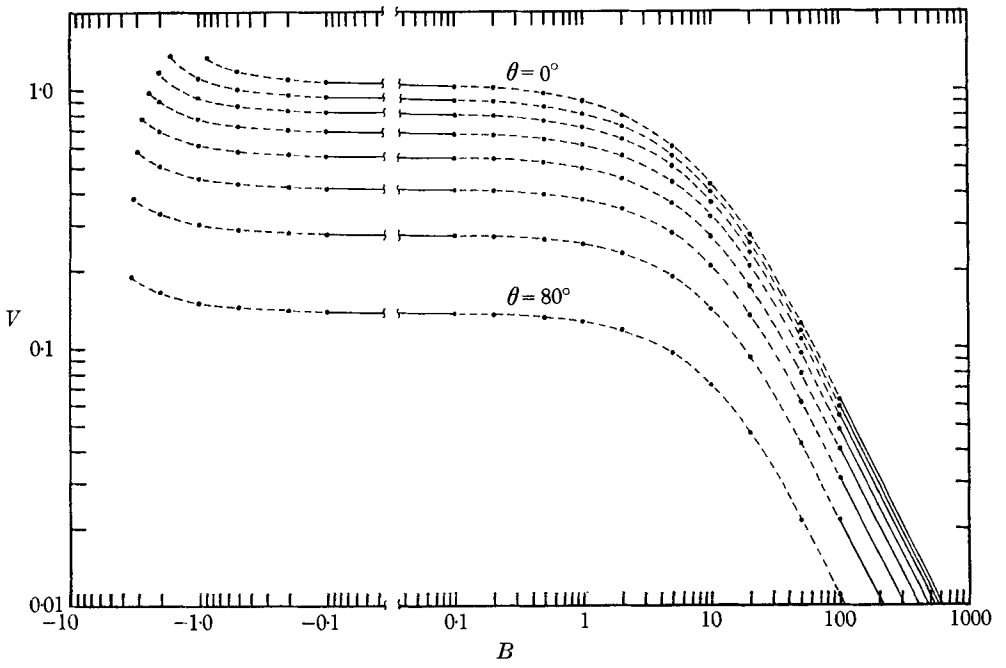

FIGURE 4. V, volume between the meniscus and the plane $z = 0$, *vs.* B, Bond number. The curves in order from top to bottom are for contact angles $\theta = 0$, 20, 30, 40, 50, 60, 70 and 80 degrees.

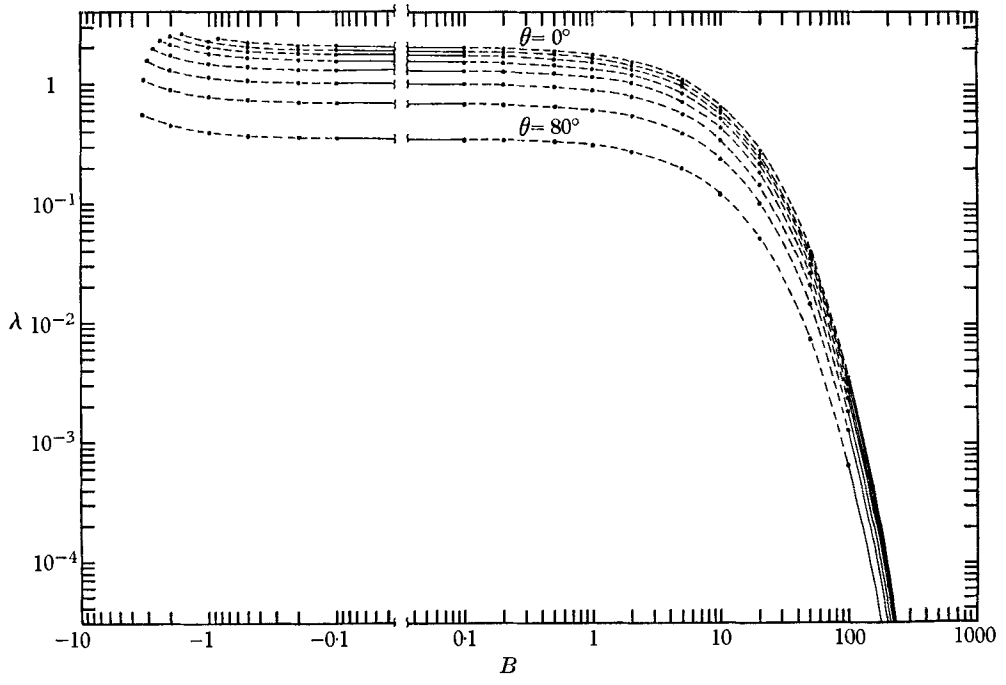

FIGURE 5. λ, twice the mean curvature at the meniscus vertex, *vs.* B, Bond number. The curves in order from top to bottom are for contact angles $\theta = 0$, 20, 30, 40, 50, 60 ,70 and 80 degrees.

small Bond numbers, and the dashed portions depict the numerical solutions calculated for intermediate Bond numbers. The heavy dots show the actual numerical values calculated—the dashed curves are faired between them. The curves are plotted on a log-log scale.

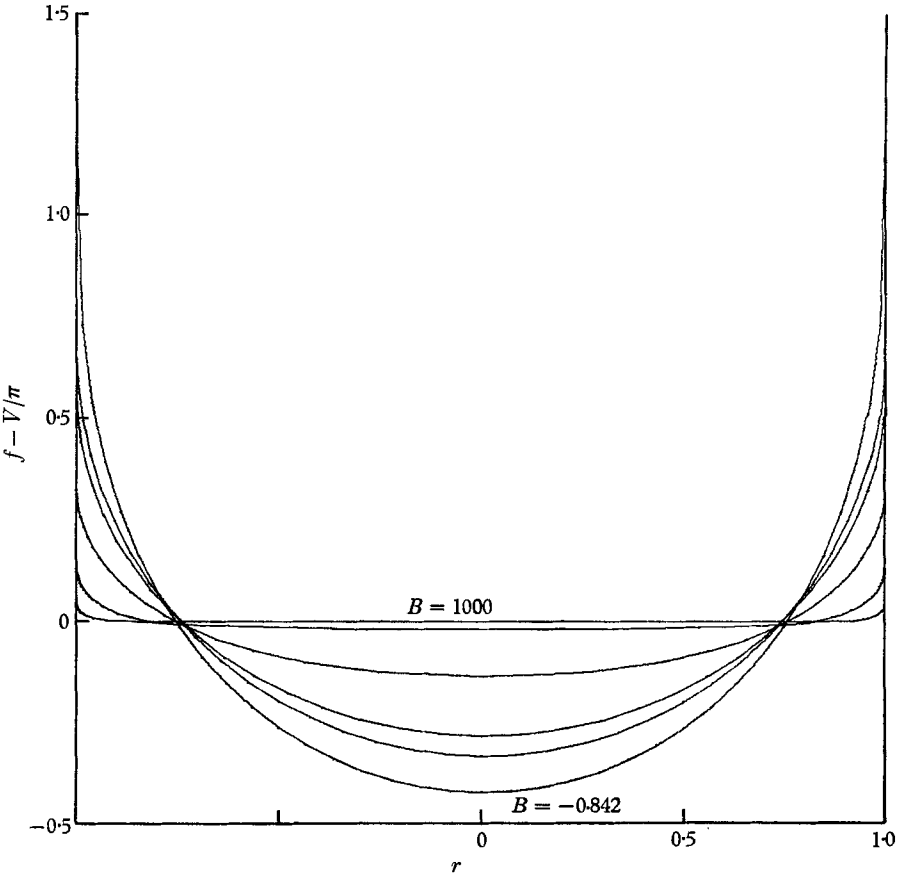

FIGURE 6. Menisci for contact angle $\theta = 0$ deg. The curves in order from the flattest to the most arched at the centre are for Bond numbers $B = 1000, 100, 10, 1, 0$ and $B_{cr} = -0{\cdot}842$.

The accuracy of the numerical solutions was checked by observing the effect of varying the mesh size, varying the value of ψ up to which (24) is used, and varying the value of D beyond which (25) is used, and by comparison with the closed-form solution for zero gravity. The numerical values of f, S, V and λ, from which the figures are prepared, were concluded to be accurate to at least six significant digits; the values of B_{cr} were determined to three digits. Comparison of the numerical solutions with those given by the asymptotic formulas showed that the asymptotic solution for small B, (8), may be used for $|B| \leqslant 0{\cdot}1$ and the asymptotic solution for large B, (12) and (15), may be used for

$$B = c^2 \geqslant 100$$

with a relative error in each case of less than 1 % in $f(\frac{1}{2}\pi - \theta)$, S, V or λ.

The curves in figures 2–5 terminate at their left-hand extremities at the critical Bond number, $B_{cr}(\theta)$, for which the curvature of f decreases to zero at the wall. These values of B_{cr} are the same as those given by Reynolds & Satterlee (figure 11.23, p. 408) to within their accuracy for the critical value of B at which

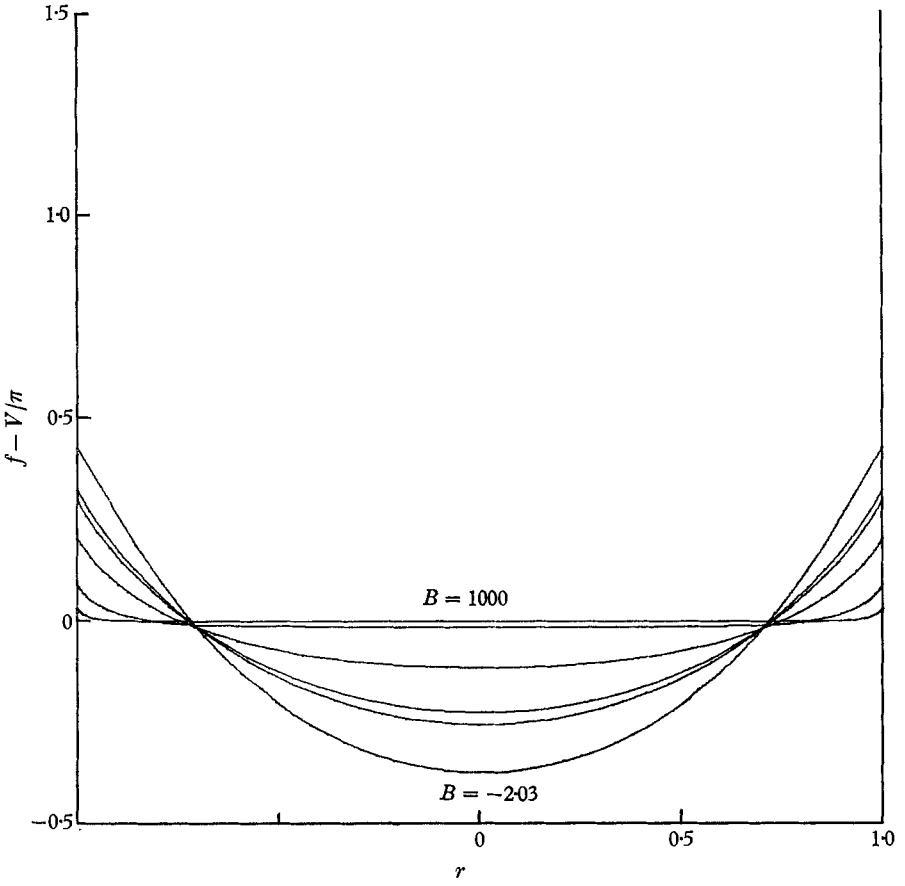

FIGURE 7. Menisci for contact angle $\theta = 30$ deg. The curves in order from the flattest to the most arched at the centre are for Bond numbers $B = 1000$, 100, 10, 1, 0 and $B_{cr} = -2{\cdot}03$.

the meniscus shape ceases to provide a stable configuration of minimum energy. Computational evidence is thus provided that the equivalence of the critical value of B at which a stable equilibrium surface is no longer possible and that at which the curvature of f just vanishes at the wall, which is the case for a two-dimensional channel (Concus 1963, 1964), holds for the cylinder also.

Figures 6–8 depict the diametral cross section of the equilibrium free surface as a function of B for $\theta = 0$, 30 and 60 deg. The curves are displaced vertically so that they all have mean height zero and correspond to the same volume of liquid.

The author expresses his appreciation to G. E. Crane, L. M. Perko and H. M. Satterlee for helpful conversations concerning this work and to R. G. Ahlstrand for obtaining computer plots of the data. This work was performed under auspices of the U.S. Atomic Energy Commission.

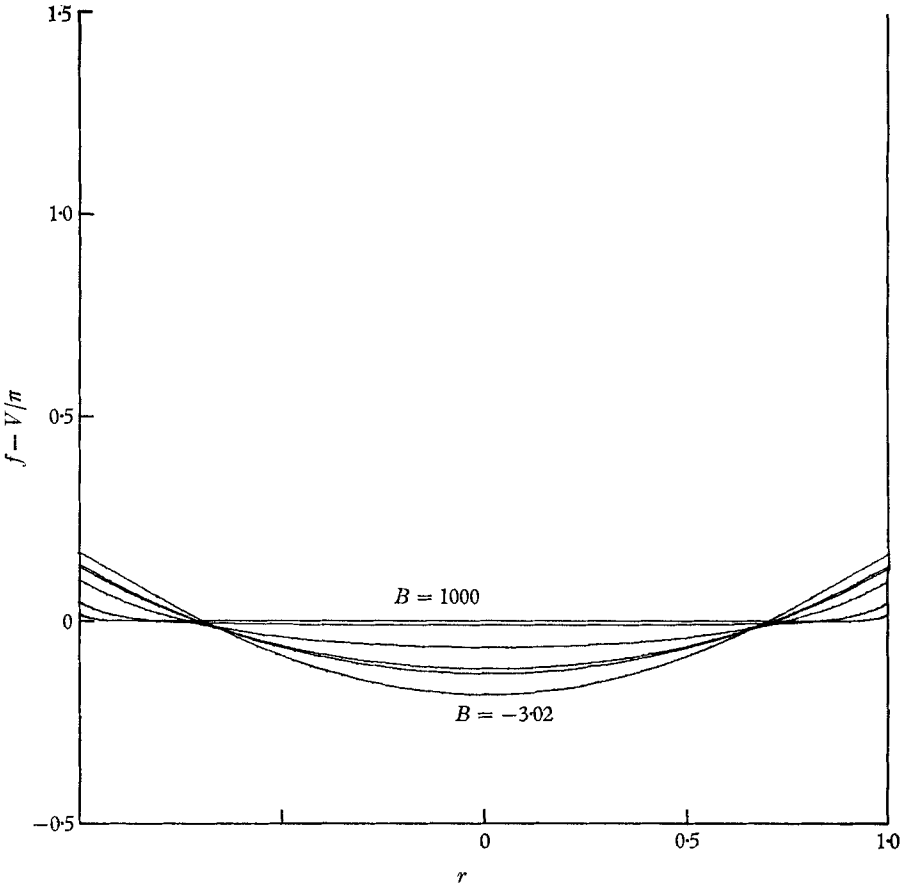

FIGURE 8. Menisci for contact angle $\theta = 60$ deg. The curves in order from the flattest to the most arched at the centre are for Bond numbers $B = 1000, 100, 10, 1, 0$ and $B_{cr} = -3{\cdot}02$.

REFERENCES

BASHFORTH, F. & ADAMS, J. C. 1883 *An Attempt to Test the Theories of Capillary Action by Comparing the Theoretical and Measured Forms of Drops of Fluid.* Cambridge University Press.

CONCUS, P. 1963 Capillary stability in an inverted rectangular tank. *Adv. Astronautical Sci.* (Western Periodicals Co., No. Hollywood, Calif.), **14**, 21–37.

CONCUS, P. 1964 Capillary stability in an inverted rectangular channel for free surfaces with curvature of changing sign. *AIAA J.* **2**, 2228–30.

FOX, L. 1962 *Numerical Solution of Ordinary and Partial Differential Equations.* Oxford: Pergamon.

HABIP, L. M. 1965 On the mechanics of liquids in subgravity. *Astronautica Acta*, **11**, 401–9.

LAPLACE, P. S. 1805 *Mécanique Céleste*, no. 4, Supplément au X^{e} Livre.

LOCKHEED MISSILES AND SPACE CO. 1967 The literature of low-g propellant behaviour. LMSC-A 874730 code Y-87-67-1.

RAYLEIGH, LORD 1916 On the theory of the capillary tube. *Proc. Roy. Soc. Lond.* A **92**, 184–95.

REYNOLDS, W. C. & SATTERLEE, H. M. 1966 Liquid propellant behavior at low and zero g. In *The Dynamic Behavior of Liquids in Moving Containers*. Ed. by H. N. Abramson. NASA SP-106, 387-439.

RUNGE, C. 1895 Über die numerische Auflösung von Differentialgleichungen. *Math. Ann.* **46**, 167–78.

WHITE, D. A. & TALLMADGE, J. A. 1965 Static menisci on the outside of cylinders. *J. Fluid Mech.* **23**, 325–35.